# Participation of macrophages in atherosclerotic lesion morphology in LDLr−/− mice[s]

**Natalie K. Schiller, Audrey S. Black, Gary P. Bradshaw, David J. Bonnet, and Linda K. Curtiss[1]**

The Scripps Research Institute, Department of Immunology, La Jolla, CA 92037

Abstract    Lyst^beige (beige) mice crossed with LDL receptor-deficient (LDLr−/−) mice had a distinct atherosclerotic lesion morphology that was not observed in LDLr−/− mice. This morphology is often associated with a stable plaque phenotype. We hypothesized that macrophage expression of the beige mutation accounted for this distinct morphology. Cultured bone marrow-derived macrophages from LDLr−/− and beige,LDLr−/− mice were compared for their ability to accumulate cholesterol, efflux cholesterol, migrate in response to chemotactic stimuli through Matrigel®-coated membranes, and express matrix metalloproteinase 9 (MMP9). No differences in cholesterol metabolism were identified. Beige,LDLr−/− macrophage invasion in vitro appeared to be less than LDLr−/− macrophage invasion but did not achieve significance. Nevertheless, tumor necrosis factor-α-induced MMP9 expression, secretion, and enzymatic activity of beige,LDLr−/− macrophages were all significantly decreased compared with those of LDLr−/− macrophages ($P < 0.05$). For in vivo analyses of macrophage function, bone marrow transplantation (BMT) studies were performed. LDLr−/− mice and beige,LDLr−/− mice were irradiated and reconstituted with wild-type or beige bone marrow from mice expressing green fluorescent protein (GFP). Identification of GFP cells provided for direct identification of donor-derived cells within lesions. Only expression of the beige mutation in the BMT recipients altered the macrophage location and collagen content of the lesions.[JLR] These results suggested that impaired macrophage function by itself did not account for the stable lesion morphology of beige,LDLr−/− double-mutant mice.—Schiller, N. K., A. S. Black, G. P. Bradshaw, D. J. Bonnet, and L. K. Curtiss. **Participation of macrophages in atherosclerotic lesion morphology in LDLr−/− mice.** *J. Lipid Res.* 2004. 45: 1398–1409.

A stable atherosclerotic lesion is generally characterized by increased collagen content, decreased macrophage foam cells, the absence of necrotic cores, and a thick smooth muscle cell or fibrous layer (1). In a previous study (2), we observed that LDL receptor-deficient (LDLr−/−) mice that expressed the beige gene (beige,LDLr−/− mice) had exacerbated atherosclerosis. In the current study, the morphology of the double mutant beige,LDLr−/− lesions were compared with that of the LDLr−/− lesions. The beige,LDLr−/− lesions had fewer lesion macrophages, greater lesion collagen content, and an apparent altered distribution of MOMA-2-staining macrophages. Mechanisms responsible for the development of those characteristics that are associated with a stable lesion as opposed to an unstable lesion are not fully understood. To identify macrophage functions that might influence lesion morphology, we examined the effect of expression of the beige mutation in macrophages in vivo and in vitro.

The beige mouse is the animal homolog of the human Chediak-Higashi syndrome (CHS) (3). The clinical symptoms of the beige/CHS mutation, such as oculocutaneous albinism and bleeding disorders, are suggested to be attributable to cellular vesicle secretion malfunction and an impairment in the exchange of membrane material between the trans-Golgi network and late endosomes (4, 5). Patients generally succumb to infections caused primarily by defective bactericidal activity of neutrophils and Natural Killer (NK) cells (5, 6). Cytotoxic T-lymphocyte, NK cell, and neutrophil activities in beige mice as well as CHS patients are defective; however, less attention has been paid to macrophage functions. Macrophages with the beige mutation have characteristic enlarged perinuclear granules as well as defective chemotaxis in vitro (7–9). Beige macrophages exhibit delays in in vitro antitumor activity similar to the delays in bactericidal activity by neutrophils, although antitumor activity is not markedly impaired in vivo (10). CHS/beige granulocytes also have reduced levels of certain lysosomal enzymes and secreted elastases (8, 9).

In bone marrow-derived cultured beige,LDLr−/− macrophages, we observed no defects in cholesterol metabo-

lism but impaired invasion and matrix metalloproteinase 9 (MMP9) expression, secretion, and activity. This suggested that invasion and/or MMP expression may contribute to the stable lesion morphology characteristic of the beige,LDLr$^{-/-}$ double-mutant phenotype. To determine in vivo if macrophages of the beige,LDLr$^{-/-}$ mice were responsible for the unique lesion morphology, we performed two bone marrow transplantation (BMT) experiments. In BMT study 1, irradiated LDLr$^{-/-}$ mice were reconstituted with either beige or wild-type bone marrow. In BMT study 2, irradiated double-mutant beige,LDLr$^{-/-}$ mice were reconstituted with either wild-type or beige bone marrow. This allowed us to study bone marrow chimerae in which only bone marrow-derived cells were beige (study 1) or all cells except bone marrow-derived cells were beige (study 2). In both studies, expression of the beige mutation in the non-bone marrow cells of the recipient had the greatest influence on lesion morphology. This suggested that expression of the beige mutation in macrophages alone was not responsible for the atherosclerotic disease phenotype of double-mutant beige, LDLr$^{-/-}$ mice. Rather, macrophages in combination with other cell types participated in the expression of a beige lesion phenotype that is more characteristic of stable lesion morphology.

## METHODS

### Animals

LDLr$^{-/-}$ mice backcrossed onto a C57Bl/6 background were purchased from Jackson Laboratories (Bar Harbor, ME) and bred in house. Double-mutant mice were generated by crossing C57Bl/6J-$Lyst^{bg-J/+}$ mice (beige), purchased from Jackson Labs, with LDLr$^{-/-}$ mice (beige,LDLr$^{-/-}$) (2). For the BMT studies, donor beige mice were crossed with mice expressing the green fluorescent protein (GFP) C57Bl/6-TgN(ACTbEGFP)10sb (beige, GFP) mice, also purchased from Jackson Labs. RT-PCR was used to genotype mice for the LDLr$^{-/-}$ mutation (2). The beige mice were phenotyped based upon coat color, and GFP expression in mice (which was under the control of a β-actin promoter) was observed under long-wavelength UV light.

The mice were weaned at 4 weeks and fed ad libitum a standard mouse chow diet (Harlan Teklad 7019). Mice used for in vitro studies were between 6 and 14 weeks old at the time of bone marrow isolation. Mice used for in vivo studies were between 8 and 10 weeks old when they were fed a high-fat, high-cholesterol diet that contained 1.25% cholesterol, 15.8% fat, and no cholate (Harlan Teklad 94059). This is referred to hereafter as the high-fat diet. Mice were fasted periodically and venous blood was drawn from the retro-orbital sinus. Plasma was isolated and total cholesterol and triglyceride levels were measured by a colorimetric method (Sigma). All mice were housed four per cage in autoclaved, filter-top cages with autoclaved water and kept on a 12 h light/dark cycle. All procedures were done in accordance with institutional guidelines.

To document lesion morphology in beige,LDLr$^{-/-}$ mice, the aortic valve sections were stained with MOMA-2 antibody to identify macrophages as described (2). Masson's trichrome stain, which stains the cytoplasm pink, collagen blue, and cell nuclei black, was used to identify collagen within the aortic sinus sections (11). Digital image analysis using Adobe Photoshop 7.0 was used to quantitate the MOMA-2-staining regions (red) and the collagen-staining regions (blue) of five heart valve sections from each animal. Each heart valve section selected for this analysis was chosen because its size was nearest the mean lesion area that had been previously determined for that individual animal. After selection of a representative color shade and intensity in a single section, the staining areas of subsequent sections with the same color shade and intensity were identified and marked using a tolerance of 30. Areas selected at this tolerance were then assigned a uniform black color, and all black pixels were counted. Digitized black pixel counts were divided by the total lesion area to arrive at the percentage staining for each section. Data presented represent means of five heart valve section measurements per mouse.

### BMT

BMT was performed as previously described (11). In the first BMT study, irradiated LDLr$^{-/-}$ mice were reconstituted with marrow from beige,GFP mice (n = 12) or wild-type GFP (wtGFP) mice (n = 12) so that only bone marrow-derived cells expressed the beige mutation. In the second BMT study, beige,LDLr$^{-/-}$ double-mutant mice were reconstituted with marrow from wt-GFP mice (n = 12) or beige,GFP mice (n = 12). This BMT study was designed so that all cells expressed the beige mutation except the bone marrow-derived cells. All BMT mice were allowed to recover from irradiation and BMT for 4 weeks. They were then fed the high-fat diet for 16 additional weeks to promote atherosclerosis.

Atherosclerotic lesion severity was assessed in the aortic sinus of the heart of the BMT mice as previously described (2). The aortic sinus lesion sections were monitored for bone marrow-derived GFP macrophage infiltration using fluorescence microscopy. Sections were mounted using Vectashield (Vector Laboratories) and observed at 488 nm using an Olympus BH2-RFCA fluorescence microscope. Green fluorescence of five sections from each mouse was assessed using Chromatica software and quantitated using NIH Scion Image software.

### Macrophage cultures

For each experiment, two LDLr$^{-/-}$ mice and two beige, LDLr$^{-/-}$ mice between 6 and 14 weeks old were euthanized in CO$_2$ and the femur and tibia of each leg were excised. Using a 23 g needle and a 1 ml syringe, the bone marrow was flushed into a sterile petri dish containing 10 ml of RPMI-1640 with 10% FBS, 2 mM L-glutamine, and 1% penicillin/streptomycin. Clumps of cells were disrupted, and the cell suspension was washed in medium. Cells were resuspended in 30 ml of low-glucose DMEM containing 30% L-929 cell (ATCC)-conditioned medium, 20% heat-inactivated fetal bovine serum, 1% penicillin/streptomycin, Glutamax®, and sodium pyruvate. This is referred to as the bone marrow growth medium. The conditioned medium from L-929 cells (a fibroblast-like cell) contains multiple growth factors (e.g., macrophage-colony stimulating factor and IFN-γ) that favor differentiation of the marrow cells into monocytes (12). The cells were seeded onto 100 mm petri dishes at 10 ml/dish (three dishes per mouse) and cultured at 37°C and 5% CO$_2$. After 3 days, medium containing nonadherent cells was removed and the adherent cells were fed with 10 ml of fresh bone marrow growth medium and cultured for 2 additional days. More than 99% of cells subcloned from the cultures were positive for CD11b and CD18 (12, 13).

At harvest, the medium was removed and the cells were washed once in 10 ml of ice-cold RPMI-1640 and incubated at 37°C in prewarmed Versene (1:5,000; Gibco). After 5 min, an equal volume of 10% FBS-RPMI medium was added to each dish and the cells were dislodged from the culture dish. Cells were counted and viability assessed by trypan blue exclusion. Cell yield and re-

covery were similar between the strains, as were cell proliferation and growth rates. These bone marrow-derived cells were used for all of the experimental systems described below.

### Bone marrow macrophage purity

The purity of our macrophage cultures was assessed by FACS analysis and the RiboQuant™ Multi-Probe RNase Protection Assay (RPA) System (Pharmingen) for mouse cell surface antigens (mCD-1) according to the manufacturer's instructions. The multiprobe template used in the RPA identified TCRδ, TCRα, CD3ε, CD4, CD8α, CD8β, CD19, F4/80, and CD45 (see supplemental fig. I).

### Cholesterol accumulation

Bone marrow-derived macrophages were diluted to $5 \times 10^5$ cells/ml in RPMI-1640 containing 1% Nutridoma-SP, 2 mM L-glutamine, 1% penicillin/streptomycin, and 50 μg/ml acetylated LDL (or no acetylated LDL for control) and seeded onto 24-well plates at 1 ml/well. Isolation and acetylation of LDL has been described previously (14). Cells were incubated for 24 h at 37°C in 5% $CO_2$. The medium was removed from the wells, clarified by centrifugation, and frozen at −20°C until it was assessed by zymography for matrix metalloproteinase activity (see below). Adherent cells were extracted at 1 ml/well for 30 min into hexane-isopropanol (3:2). The lipid extracts were removed from the well, dried down in glass tubes, and stored at −20°C for further lipid analysis by thin layer chromatography as described previously (15). After lipid extraction, cells were lysed for 30 min with 0.1 N NaOH at 0.5 ml/well. Lysates were stored at −20°C for protein analysis by a modified Lowry method (16).

### Cholesterol efflux assay

Bone marrow macrophages were diluted to $5 \times 10^5$ cells/ml in 1% Nutridoma-SP medium containing 50 μg/ml acetylated LDL (acLDL) and 1 μCi/ml NET-725-cholesterol [1,2,6,7-3H(N)] (1.0 mCi/ml; New England Nuclear). Cells were seeded on 24-well plates in triplicate and incubated for 20 h at 37°C in 5% $CO_2$. Medium was removed and cells were allowed to equilibrate for 1 h in 1% Nutridoma-SP medium. After equilibration, cells were treated at 37°C with 10 μg/ml human apolipoprotein A-I (apoA-I) in 1% Nutridoma-SP medium or with medium alone for 4 and 24 h (17). Supernatants were collected and centrifuged at 10,000 rpm for 10 min. Cells were washed once in PBS and lysed in 1 ml of 0.1 N NaOH. Aliquots of supernatants and cell lysates were counted.

### Macrophage invasion

Bone marrow-derived macrophages were diluted in either 5% FBS-DMEM or DMEM alone to $2.5 \times 10^5$ cells/ml. Cell suspensions were added in triplicate to rehydrated Matrigel® inserts (BD-Biocoat) and transferred to wells containing mouse JE/CCL2 (JE/MCP-1; R and D Systems) (0.03 μg/ml) in 5% FBS-DMEM or DMEM with no chemoattractant. Matrigel® inserts were incubated for 20 h at 37°C and 5% $CO_2$. Cell suspensions were aspirated from the insert, and nonadherent cells were vigorously removed with a cotton swab. Matrigels® were removed from inserts and mounted on microscope slides. Three fields per gel at 10× magnification were digitized, and cells per field were counted. The average of the three fields was calculated. Each data point represents the average of three Matrigel® wells per culture. Matrigels® incubated in the absence of chemoattractant consistently had between 0 and 30 cells migrating.

### Zymography

Bone marrow-derived macrophages were diluted to $5 \times 10^5$ cells/ml in RPMI-1640 containing 1% Nutridoma-SP, 2 mM L-glutamine, and 1% penicillin/streptomycin and seeded onto
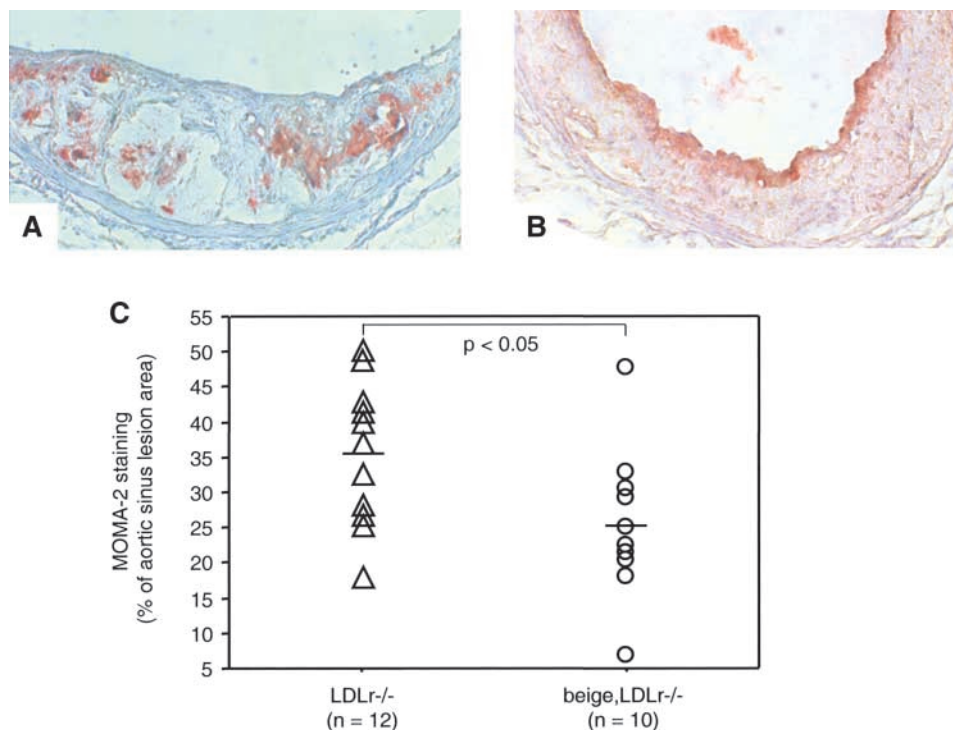


Fig. 1. Cellular morphology of double-mutant mice as assessed by infiltration of MOMA-2-positive macrophages in the aortic sinus lesions of LDL receptor-deficient (LDLr$^{-/-}$; A) or beige,LDLr$^{-/-}$ (B) mice. Magnification, 200×. C: MOMA-2-positive cells were quantified by digital imaging software as described in Methods and are reported as percentage staining per total lesion area.

24-well plates at 1 ml/well. Cells were allowed to adhere overnight. Medium was replaced with fresh 1% Nutridoma-SP medium containing tumor necrosis factor-$\alpha$ (TNF-$\alpha$; 1 ng/ml) or no treatment and incubated for 24 h at 37°C and 5% CO$_2$. Supernatants were collected, cleared, and stored at $-20$°C. Cells were washed once with PBS and then lysed in 1 ml of 0.1 N NaOH. Protein concentrations of cell lysates were determined using the MicroBCA™ Protein Reagent Kit (Pierce, Rockford, IL). The supernatants were denatured in SDS and separated on precast 12-well, 10% polyacrylamide gels containing 0.1% gelatin (Novex) according to the manufacturer's instructions. Clearing of gels was analyzed by ImageQuant software and was normalized to cell lysate protein concentrations.

To confirm that gel clearing was attributable to MMP activity, the serine protease inhibitor PMSF (1 mM) or the metal chelator EDTA (20 mM) was added to the developing buffer. Activation of the pro form of the enzyme was achieved by incubating supernatants overnight at 37°C in 2 mM $p$-aminophenylmercuric acetate (APMA). To confirm the presence of MMP9, supernatants underwent immunoprecipitation clearing before zymography. We incubated supernatants with rabbit anti-mouse MMP9 polyclonal antibodies (Chemicon International). Immune complexes were immunoprecipitated with rabbit IgG antibodies conjugated to agarose beads (Novus Biologicals). Beads were pelleted by centrifugation, and supernatants were tested for activity by zymography. MMP9 protein in the supernatants was measured by ELISA using a Quantikine™ M Mouse pro-MMP9 immunoassay according to the manufacturer's instructions (R and D Systems).

### MMP9 gene expression

Bone marrow-derived macrophages were cultured as described above. On day 5, the bone marrow growth medium was replaced with DMEM containing 1 mM L-glutamine, 1% penicillin/streptomycin, and 1% Nutridoma-SP. Cells were cultured overnight in the serum-free medium and cultured for an additional 24 h with or without 20 ng/ml TNF-$\alpha$. Total RNA was isolated using Trizol reagent. RNA (5 $\mu$g/lane) was loaded onto a 1% formaldehyde-agarose gel, electrophoresed, and blotted onto a positively charged nylon membrane. Blots were probed with a $^{32}$P-labeled cDNA probe for MMP9 (1.4 kb). Hybridization was carried out at 42°C and washing at 65°C. Blots were then stripped and reprobed with a $^{32}$P-labeled $\beta$-actin probe from Ambion (DECA template $\beta$-actin).

### Statistics

All results were expressed as means $\pm$ SD except where noted. All lesion data were analyzed by the Mann-Whitney test, and all other analyses used an unpaired $t$-test in the Statview SE+ statistics package (SAS Institute, Inc., Cary, NC). $P < 0.05$ was considered significant.

## RESULTS

We previously reported that double-mutant beige, LDLr$^{-/-}$ mice have exacerbated atherosclerosis compared with LDLr$^{-/-}$ controls (2). Here, we document the distinct morphology of the aortic sinus lesions of these mice. **Figure 1** illustrates the unique distribution of macrophages within the aortic sinus of beige, LDLr$^{-/-}$ mice compared with LDLr$^{-/-}$ mice. In these double-mutant mice, macrophages were localized to the lumenal surface
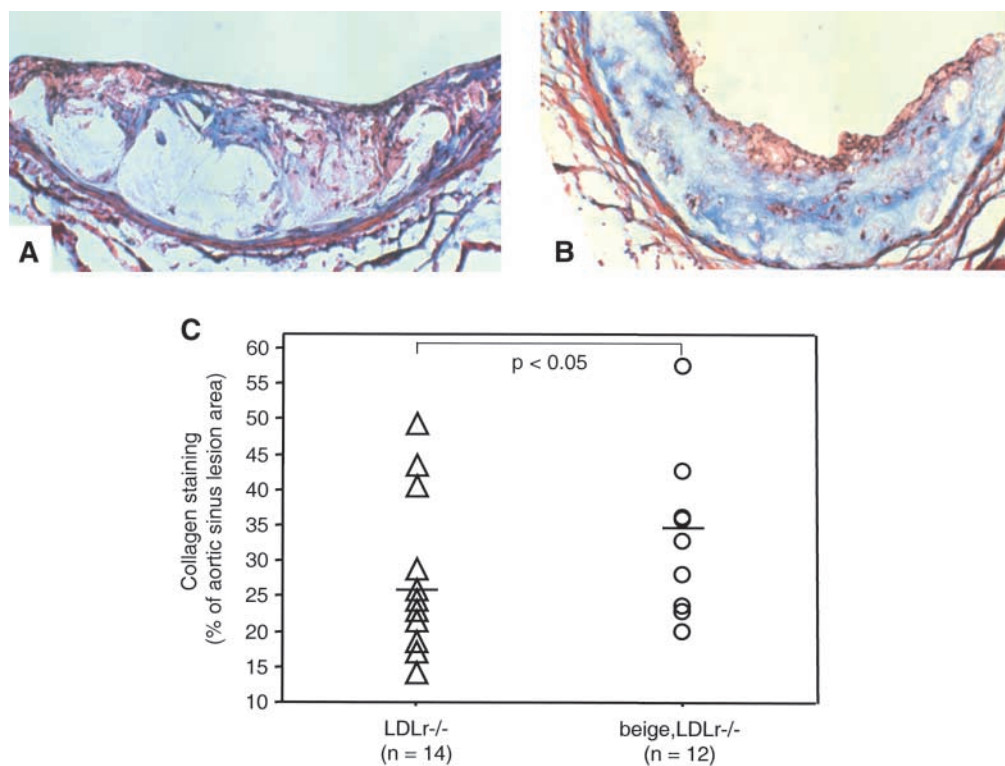


**Fig. 2.** Collagen content of aortic sinus lesions from double-mutant mice as assessed by Masson's trichrome-staining LDLr$^{-/-}$ (A) and beige,LDLr$^{-/-}$ (B) mice. Magnification, 200×. C: Collagen content of LDLr$^{-/-}$ (triangles) and beige,LDLr$^{-/-}$ (circles) aortic sinus lesions was quantitated as described in Methods using digital imaging software. Data are reported as percentage of the total lesion area that stained blue for collagen.

of the lesions (Fig. 1B), whereas LDLr$^{-/-}$ mice had lesions with MOMA-2 staining throughout the interior as well as on the lumenal surface (Fig. 1A). Quantitation of the MOMA-2-positive staining of sections from multiple mice revealed the presence of significantly fewer macrophages in the lesions of the beige, LDLr$^{-/-}$ mice (Fig. 1C). This suggested that the beige mutation may affect macrophage survival or movement into and/or out of lesions.

Another characteristic of the lesions in the double-mutant mice was the sparse presence of lipid cores that was accompanied by a denser extracellular matrix. **Figure 2A, B** shows aortic sinus lesions stained with Masson's trichrome to assess collagen content (blue). Beige,LDLr$^{-/-}$ double-mutant mice had lesions with fewer lipid cores and a more uniform and dense collagen matrix compared with LDLr$^{-/-}$ mice. To document this difference, the collagen content of beige,LDLr$^{-/-}$ lesions was digitally quantified and found to be significantly increased compared with that of LDLr$^{-/-}$ mice (Fig. 2C). These histologic analyses suggested that the beige mutation may influence both matrix turnover and macrophage infiltration. Therefore, we characterized both in vitro and in vivo the beige,LDLr$^{-/-}$ phenotype of bone marrow-derived macrophages.

### Effect of the beige mutation on in vitro macrophage functions

We compared cultured bone marrow-derived macrophages that were isolated from LDLr$^{-/-}$ and beige, LDLr$^{-/-}$ mice. Calculation of the cell yield per mouse after culture in L-929-conditioned medium for 5 days demonstrated no gender or congenic strain differences. There were, however, slight differences in cell yields from all mice between the ages of 5 and 9 weeks compared with mice between the ages of 11 and 15 weeks ($P = 0.06$; $1.01 \times 10^7$ cells/5–9 week old mice vs. $7.9 \times 10^6$ cells/11–

15 week old mice). The purity of the macrophage cultures was assessed by RPA. The cultured macrophage gave bands only for F4/80 (a macrophage marker) and CD45 (a hematopoietic marker) (see supplemental fig. I). This confirmed that the cultures were predominantly macrophage and contained few other contaminating cells.

The decreased incidence of lipid-rich necrotic cores and foam cells within the lesions of beige,LDLr$^{-/-}$ mice suggested that beige mutant macrophages might have altered cholesterol metabolism. Lipid accumulation was assessed by thin layer chromatography of free cholesterol and cholesteryl esters after a 24 h labeling period of the macrophages in the presence of 50 μg/ml acLDL. Baseline levels of cholesteryl esters (**Fig. 3A**) and free cholesterol (Fig. 3B) were comparable between LDLr$^{-/-}$ and beige,LDLr$^{-/-}$ macrophages. Upon addition of acLDL, there was a comparable increase in free cholesterol and cholesteryl esters, suggesting that the beige mutation does not alter cholesterol accumulation.

Cholesterol efflux also was assessed in the LDLr$^{-/-}$ and beige,LDLr$^{-/-}$ macrophages (**Fig. 4**). Bone marrow-derived macrophages were preloaded by incubation for 20 h with 1 μCi of [$^3$H]cholesterol and 50 μg/ml acLDL. Efflux of cholesterol was assessed after 4 and 24 h of exposure to lipid-free apoA-I. Cholesterol efflux from beige, LDLr$^{-/-}$ macrophages was comparable to that from LDLr$^{-/-}$ control macrophages after both 4 and 24 h.

Invasion of neutrophils and monocytes into tissues has been suggested to be impaired in beige mutant mice (18, 19). Moreover, localization of the MOMA-2 staining of beige,LDLr$^{-/-}$ lesions to the lumenal surface suggested a possible impairment in macrophage invasion. Therefore, invasion of the bone marrow-derived macrophage across a simulated basement membrane in response to the CCR2 chemokine JE/MCP-1 was examined (**Fig. 5**). Invasion of beige,LDLr$^{-/-}$ macrophages in response to 0.03 μg/ml JE/MCP-1 appeared impaired in individual experiments.
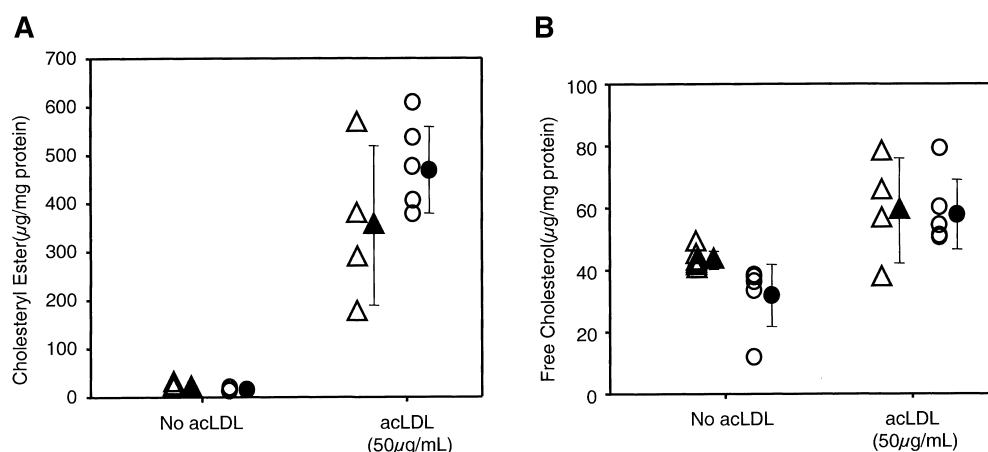


**Fig. 3.** Accumulation of cholesteryl esters (A) and free cholesterol (B) in cultured bone marrow-derived macrophages after 24 h of exposure to 50 μg/ml acetylated LDL (acLDL). LDLr$^{-/-}$ (triangles) and beige,LDLr$^{-/-}$ (circles) macrophages. Data are reported as micrograms per milligram of cell protein. The means and standard deviations of multiple experiments are shown next to each scatterplot. n = 6 experiments, except n = 4 for acLDL-treated LDLr$^{-/-}$ macrophages.
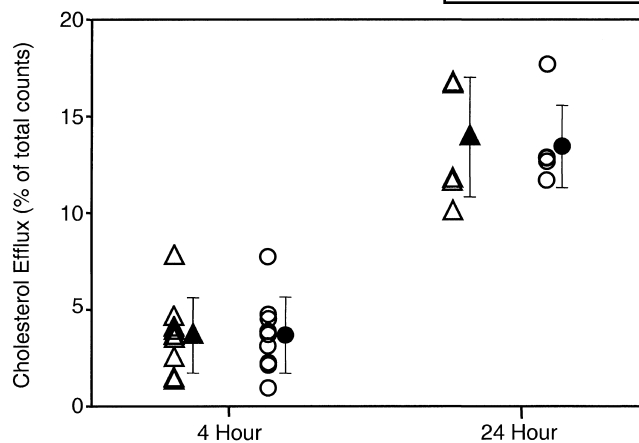
**Fig. 4.** Cholesterol efflux of bone marrow-derived macrophages after 4 and 24 h of incubation in medium containing 10 μg/ml apolipoprotein A-I. LDLr$^{-/-}$ (triangles) and beige,LDLr$^{-/-}$ (circles) mice. The means and standard deviations are shown next to each scatterplot. n = 9 experiments for the 4 h time point and n = 6 experiments for the 24 h time point.

Collectively, however, this difference was not significant ($P = 0.32$) and this was likely attributable to the large interassay variation. When the data from six different experiments were pooled, it was evident that beige,LDLr$^{-/-}$ macrophages were equally capable of transversing a Matrigel® matrix in response to CCR2 chemokine exposure.

Multiple phases of atherosclerosis are influenced by MMPs (20, 21). MMPs influence the transmigration of leukocytes as well as the collagen balance of lesions. Therefore, the altered macrophage distribution as well as the increased percentage of the aortic sinus lesion area that stained positive for collagen of beige,LDLr$^{-/-}$ mice (Fig. 2) may have been attributable to impaired macrophage secretion of matrix-degrading enzymes. Macrophages secrete MMP9 in response to TNF-α (22). We therefore compared TNF-α-induced MMP9 mRNA expression, protein secretion, and activity of cultured macrophage from LDLr$^{-/-}$ and beige,LDLr$^{-/-}$ mice. **Figure 6A** shows a typical experiment with a single band of gelatin clearing (at ~100 kDa) that was induced by exposure of the macrophage to increasing doses of TNF-α. This was indicative of pro-MMP9 activity. This activity was significantly decreased ($P = 0.03$ vs. LDLr$^{-/-}$) in beige,LDLr$^{-/-}$ macrophages compared with LDLr$^{-/-}$ macrophages upon exposure to 1 ng/ml TNF-α (Fig. 6B). We confirmed that the band of clearing was a matrix metalloproteinase by its sensitivity to EDTA, its insensitivity to PMSF, and its activation by APMA (data not shown). Moreover, the activity of the secreted protein was inhibited by an anti-MMP9 antiserum that contained antibodies that recognized both latent and active forms of the enzyme.

The concentration of pro-MMP9 antigen in the supernatants of the cultured macrophages was quantified by ELISA (**Fig. 7**). Baseline levels of pro-MMP9 were similar between LDLr$^{-/-}$ and beige,LDLr$^{-/-}$ macrophages. However, upon TNF-α exposure, the amount of secreted pro-

MMP9 from beige,LDLr$^{-/-}$ macrophages was significantly less than ($P = 0.007$) that from LDLr$^{-/-}$ macrophage. Thus, pro-MMP9 secretion was impaired in beige,LDLr$^{-/-}$ macrophages.

Finally, MMP9 expression was assessed by Northern blot analysis (**Fig. 8**). Compared with LDLr$^{-/-}$ bone marrow-derived macrophages, beige,LDLr$^{-/-}$ macrophages stimulated with 20 ng/ml TNF-α had an attenuated induction of MMP9 expression ($P < 0.05$). There also appeared to be a reduction in the baseline level of MMP9 expression in bone marrow-derived macrophages from beige,LDLr$^{-/-}$ mice compared with those isolated from LDLr$^{-/-}$ mice. However, this reduction was not statistically significant in that the overall level of baseline expression in the non-stimulated macrophages was minimal.

## Effect of the beige mutation on atherosclerotic lesion morphology

Two BMT studies were performed to examine macrophage expression of the beige mutation in vivo. Growth rates and plasma total cholesterol levels were similar in all BMT mice (see supplemental fig. II). Using aortic sinus lesions, the effect of macrophage expression of the beige mutation on lesion morphology was examined. This was accomplished by observing the localization of macrophages in the intima, the total macrophages, and the collagen content of the lesions and the area of the lipid cores. A comparison of panels A and B (BMT 1) with panels C and D (BMT 2) in **Fig. 9** suggests that the major determining factor in macrophage localization was not the genotype of the BMT donors but the genotype of the BMT recipients. Compared with all LDLr$^{-/-}$ recipients, the GFP bone marrow cells of the beige,LDLr$^{-/-}$ recipients were localized predominantly in a subluminal pattern and not uniformly throughout the intima. Total GFP-positive cells were quantified in all lesions and expressed as a percentage of the total aortic sinus lesion area. No signifi-
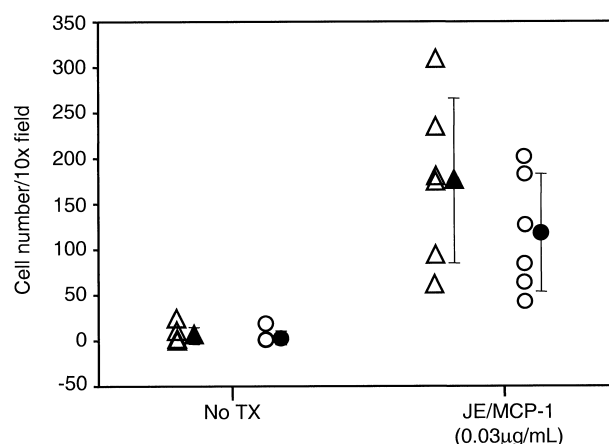


**Fig. 5.** Invasion of bone marrow macrophages through an 8 μm pore Matrigel® in response to 0.03 μg/ml JE/MCP-1. LDLr$^{-/-}$ (triangles) and beige,LDLr$^{-/-}$ (circles) macrophages. Data are reported as cell numbers per 10× field. Three fields were counted per well and three wells per experiment. n = 6 experiments. TX, treatment.
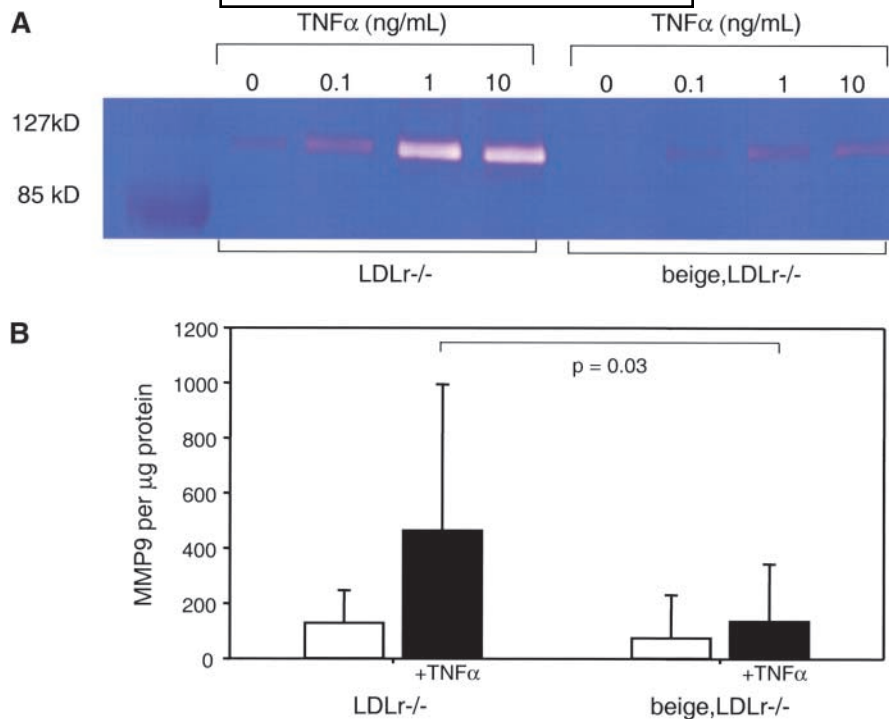
**Fig. 6.** Secreted matrix metalloproteinase activity of supernatants from LDLr$^{-/-}$ (first bars) and beige,LDLr$^{-/-}$ (second bars) cultured macrophages treated with increasing doses of tumor necrosis factor-$\alpha$ (TNF-$\alpha$; ng/ml). A: Zymogram showing the dose response of TNF-$\alpha$ on pro-matrix metalloproteinase 9 (pro-MMP9) activity. B: Pro-MMP9 activity of macrophages treated with TNF-$\alpha$ (1 ng/ml) or no treatment (n = 6). Data are reported as clearing per microgram of cell protein.

cant quantitative differences were observed between the LDLr$^{-/-}$ or beige,LDLr$^{-/-}$ mice reconstituted with beige, GFP or wtGFP bone marrow (**Fig. 10**). Thus, the numbers of bone marrow-derived cells in all of the lesions were comparable, although the localization did not appear to be comparable (Fig. 9).
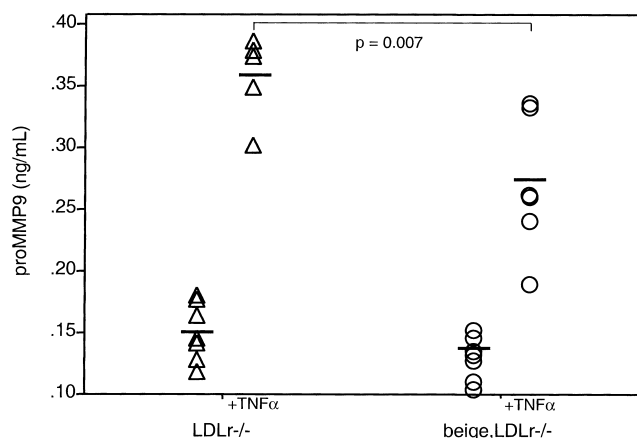


**Fig. 7.** Pro-MMP9 concentration of supernatants from untreated bone marrow-derived macrophages or macrophages treated with 1 ng/ml TNF-$\alpha$. LDLr$^{-/-}$ macrophage (triangles) and beige,LDLr$^{-/-}$ (circles). Data are reported as nanograms of pro-MMP9 per milliliter. n = 8 experiments for untreated and n = 6 experiments for TNF-$\alpha$ exposure.

In double-mutant beige,LDLr$^{-/-}$ mice, the mean percentage of the aortic sinus lesions that stained positively with MOMA-2 was ~35% compared with 25% for LDLr$^{-/-}$ mice (Fig. 1). In our BMT studies, we used GFP fluorescence to identify bone marrow-derived cells (Fig. 9), and these cells represented only 4–8% of the total lesion area. Although it is inappropriate to compare irradiated BMT mice (Fig. 9) with nonirradiated mice (Fig. 1) (11), our studies suggest that MOMA-2 staining and GFP fluorescence do not measure identical cell populations and cannot be directly compared.

Lesions of BMT mice were assessed by Masson's trichrome for collagen content. The collagen content of aortic sinus lesions was quantified, and no differences were observed in LDLr$^{-/-}$ recipients regardless of bone marrow received (**Fig. 11A, B**). However, the total collagen content of the lesions of the beige,LDLr$^{-/-}$ recipients was greater than that of the LDLr$^{-/-}$ recipients (**Fig. 12**). Also evident in Fig. 11 is the presence of smaller lipid cores in the beige,LDLr$^{-/-}$ recipients. Therefore, the aberrant macrophage functions characteristic of the beige mutation that were identified in vitro did not affect matrix turnover or cellular infiltration in vivo in the BMT model. Instead, the data strongly suggested that other cell types expressing the beige mutation contributed to the increased collagen content.

Both LDLr$^{-/-}$ mice and beige,LDLr$^{-/-}$ mice reconstituted with beige bone marrow had smaller lesion areas

**A**



MMP9

β-actin

No tx    TNFα (20ng/mL)    No tx    TNFα (20ng/mL)

**B**



p < 0.05

Ratio MMP9/β-actin
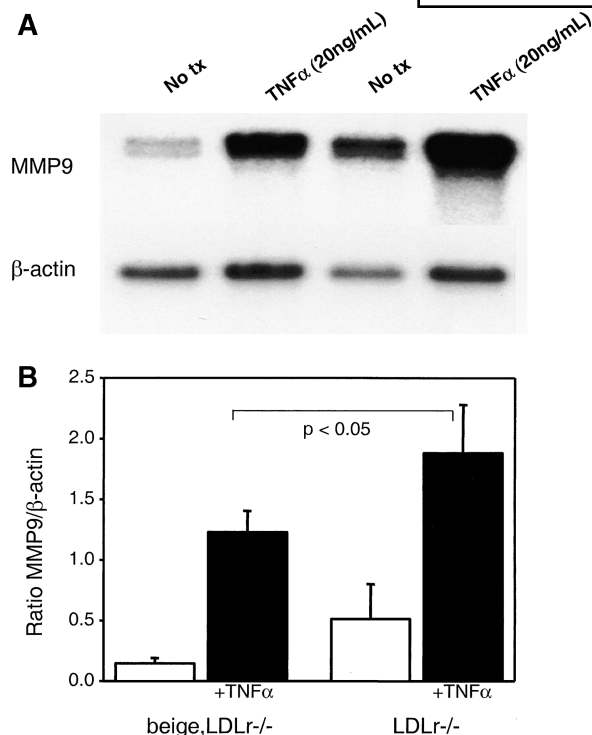
+TNFα          +TNFα
beige,LDLr-/-    LDLr-/-

**Fig. 8.** MMP9 expression in bone marrow-derived macrophages untreated (No tx) or treated with TNF-α (20 ng/ml). A: Representative Northern blot showing MMP9 expression and β-actin expression. Beige,LDLr$^{-/-}$ macrophage data are shown in the left two bars and LDLr$^{-/-}$ macrophage data are shown in the right two bars. B: Ratio of MMP9 expression to β-actin expression in bone marrow-derived macrophages. n = 3 experiments.

than the same mice reconstituted with nonmutant bone marrow. In BMT study 1 (**Fig. 13A**), expression of the beige mutation only in macrophages in LDLr$^{-/-}$ mice significantly reduced lesion area. In BMT study 2 (Fig. 13B), expression of the beige mutation in every cell except macrophages also significantly reduced lesion area. These BMT studies demonstrated that beige macrophages alone cannot account for the increased disease severity observed and reported previously (2) in nonirradiated and non-BMT double-mutant beige,LDLr$^{-/-}$ mice. Moreover, we reported previously (11) that the aortic sinus lesions of irradiated and bone marrow-transplanted LDLr$^{-/-}$ mice differ from those of LDLr$^{-/-}$ mice that are not exposed to irradiation. Therefore, direct comparisons cannot be made between studies of double-mutant beige,LDLr$^{-/-}$ mice and BMT beige,LDLr$^{-/-}$ mice. Nevertheless, these studies clearly suggest that expression of the beige mutation by additional cell types, including smooth muscle cells and endothelial cells, is involved in disease severity and lesion morphology.

## DISCUSSION

Erosion, ulceration, or rupture of the surface of atherosclerotic plaques exposes highly thrombogenic components within the interior of the lesion. Vascular smooth muscle cell (VSMC) and macrophage apoptosis, loss of extracellular matrix integrity, and inflammatory cell accumulation in the fibrous cap are thought to be important
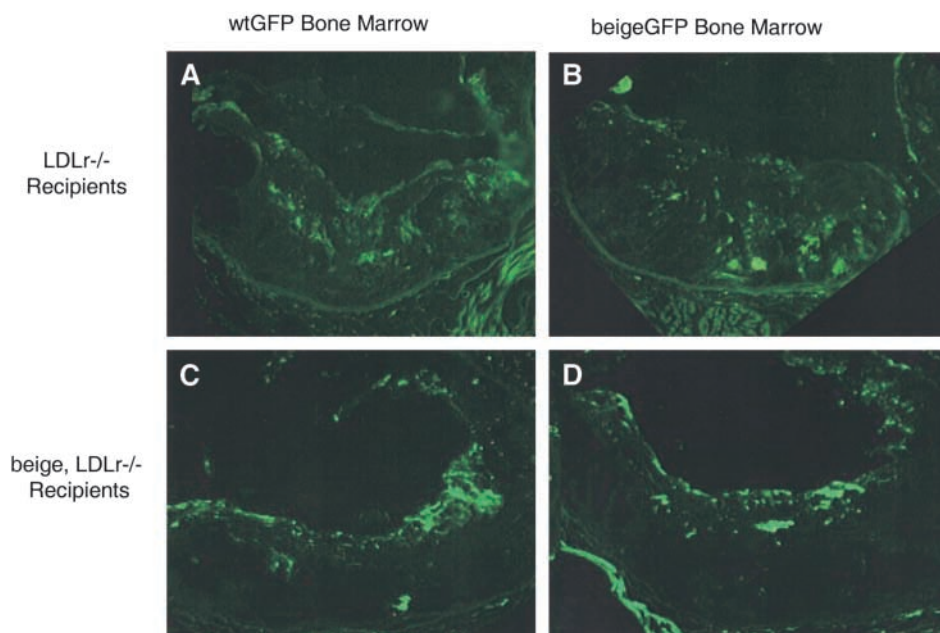


wtGFP Bone Marrow          beigeGFP Bone Marrow

LDLr-/-
Recipients

beige, LDLr-/-
Recipients

**Fig. 9.** Atherosclerosis in the aortic sinus of LDLr$^{-/-}$ (A, B) and beige,LDLr$^{-/-}$ (C, D) recipients reconstituted with wild-type green fluorescent protein (wtGFP; A, C) or beige,GFP (B, D) bone marrow. Each field contains a single lobe and is oriented with the lumen at the top. Penetration of bone marrow-derived macrophages into the lesions was revealed by fluorescence microscopy.
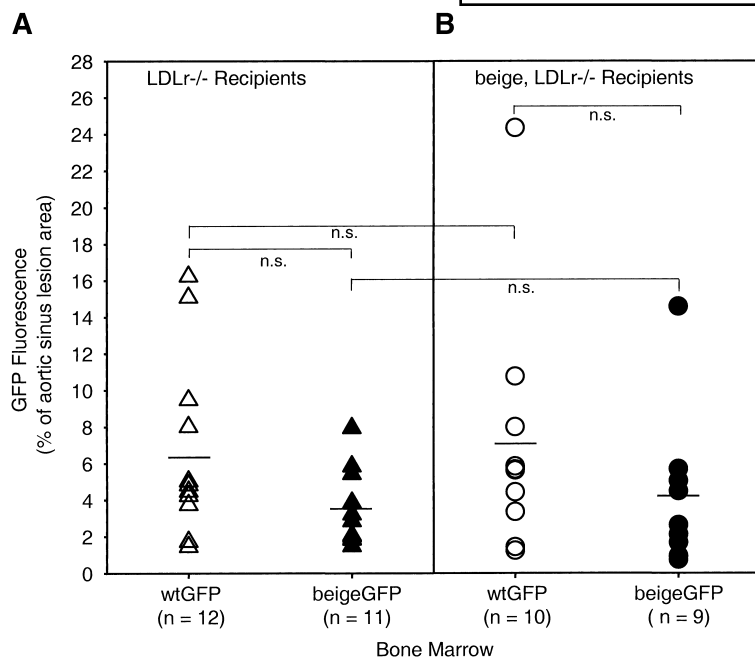
**Fig. 10.** Quantitation of GFP fluorescence in the aortic sinus lesions of bone marrow transplantation (BMT) LDLr$^{-/-}$ mice (A) or beige,LDLr$^{-/-}$ mice (B) reconstituted with wtGFP (open triangles, open circles) or beige,GFP (closed triangles, closed circles) bone marrow. The high-fat diet was initiated 4 weeks after BMT, and mice were fed this diet for 16 weeks until the time of death. Data are reported as percentage of fluorescence per total lesion area after quantitation by digital imaging. n.s., not significant.

pathogenic factors leading to lesion instability (23). Attempts to produce an animal model for plaque rupture have proved difficult. Atherosclerotic lesions in mice generally are regarded as resistant to rupture. However, Johnson and Jackson (24) reported that apoE$^{-/-}$ mice fed a high-fat diet for at least 1 year exhibited occlusive thrombus formation in the brachiocephalic (innominate) artery. Histologic examination of these vessels showed thin caps, loss of plaque VSMCs, and hemorrhage. The location of these ruptured lesions was specific to the brachiocephalic trunk. Rosenfeld et al. (25) reported that apoE$^{-/-}$ mice fed a chow diet for 42 weeks exhibited a high frequency of

lesion hemorrhage in the innominate artery that was accompanied by loss of the fibrous cap and fibrotic conversion of the necrotic core. By 60 weeks, thin fibrous caps were present with a discontinuous endothelium and occasional exposed macrophage foam cells, suggestive of lesion erosion. These studies indicate that vulnerable lesions, although difficult to produce, are observed in mice.

Our previous studies of the role of NK cells in atherosclerosis were performed in LDLr$^{-/-}$ mice that were crossed with severely NK cell-deficient beige mutant mice (2). When the LDLr$^{-/-}$ and beige,LDLr$^{-/-}$ aortic sinus lesions were compared, striking differences in lesion mor-
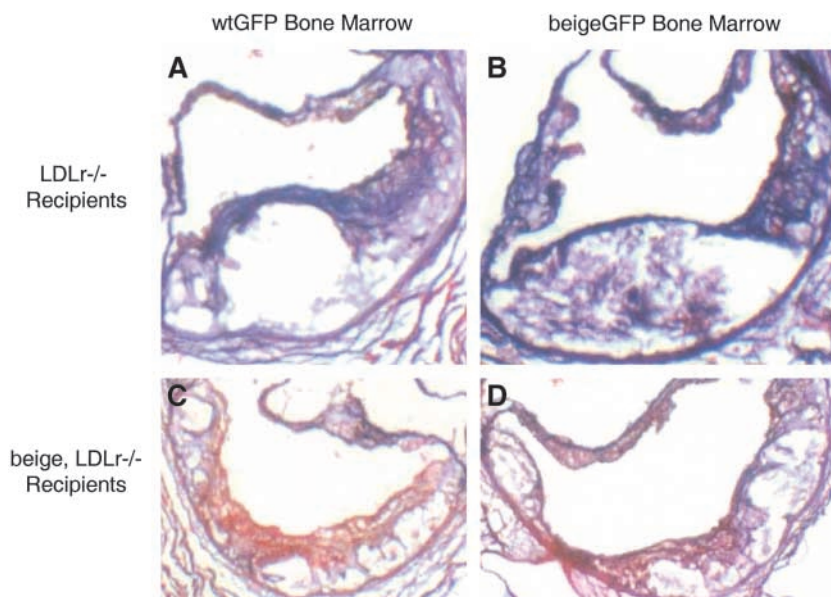


**Fig. 11.** Lesion morphology as assessed by collagen staining of aortic sinus lesions of LDLr$^{-/-}$ or beige,LDLr$^{-/-}$ BMT recipient mice reconstituted with wtGFP or beige,GFP. Magnification, 200×. Lumen is shown at top.
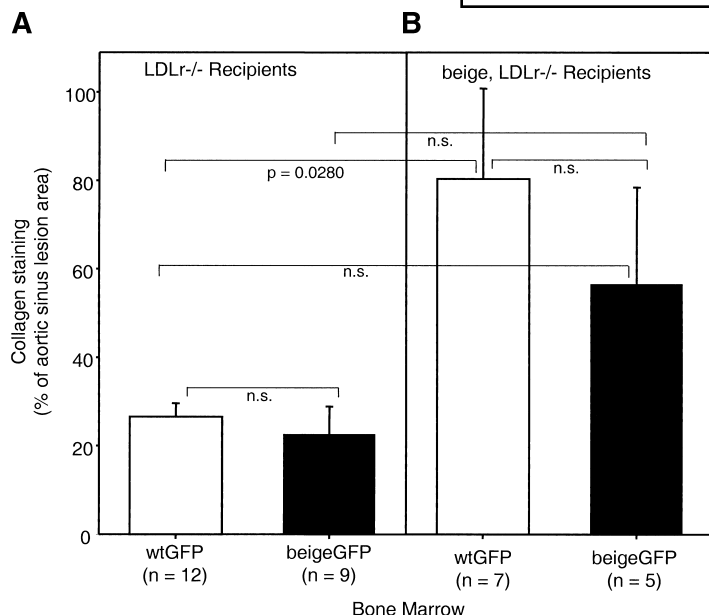
**A** **B**



**Fig. 12.** Quantitation of collagen content as assessed by Masson's trichrome staining of the aortic sinus lesions of LDLr$^{-/-}$ and beige,LDLr$^{-/-}$ mice reconstituted with wtGFP (open bars) and beige,GFP (closed bars) bone marrow cells. Collagen-positive cells were observed by microscopy and quantitated by digital imaging software. The data are reported as percentage of collagen staining per total lesion area. n.s., not significant.

phology were observed. The lesion macrophages in the beige,LDLr$^{-/-}$ mice were fewer and were confined to the luminal surface of the intima. Large necrotic cores were absent. Instead, VSMCs occupied a larger portion of the intima that was rich in collagen. These features of the lesions in beige,LDLr$^{-/-}$ mice are characteristic of a more stable lesion phenotype. More importantly, these features can be studied in beige,LDLr$^{-/-}$ mice within reasonable periods of time. We therefore sought to identify specific macrophage functions that contributed to the development of a stable-lesion phenotype.

The importance of macrophages in atherosclerosis was established by studies of op/op mice (26–28). These mice lack macrophage-colony stimulating factor and are severely deficient in circulating monocytes as well as tissue macrophages. Crossing these mice with apoE$^{-/-}$ or LDLr$^{-/-}$ mice results in little or no macrophage infiltration or atherosclerosis. Based upon these observations as well as the fact that macrophages secrete numerous growth factors and chemokines that further promote cellular accumulation in lesions, macrophages are generally considered to be proatherogenic. The BMT experiments in this study were designed to identify the effect of macrophage functions on lesion morphology.

The beige protein is involved in cellular vesicle formation and trafficking (5). This could affect macrophage cholesterol metabolism and trafficking. Furthermore, the lesions of the double-mutant beige,LDLr$^{-/-}$ mice exhibited fewer lipid cores and foam cells. This may have been attributable to impaired cholesterol metabolism in beige,
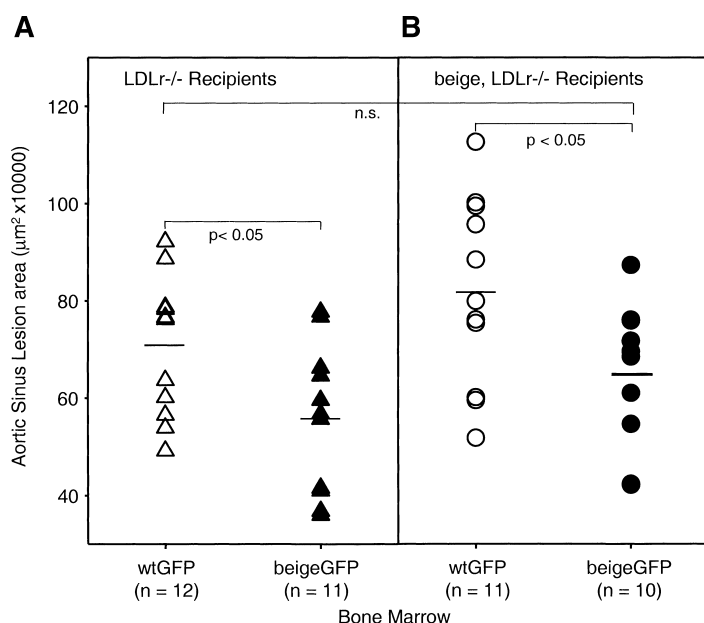
**A** **B**



**Fig. 13.** Comparison of the extent of lesion areas of BMT study 1 and BMT study 2. Atherosclerosis in the aortic sinus lesions of LDLr$^{-/-}$ (A) or beige,LDLr$^{-/-}$ (B) mice reconstituted with wtGFP (open triangles, open circles) or beige GFP (closed triangles, closed circles). Data are reported as area per square micrometer for individual mice. n.s., not significant.

LDLr$^{-/-}$ mice. However, upon exposure to acLDL, cellular free cholesterol as well as the cholesteryl ester contents of cultured beige,LDLr$^{-/-}$ and LDLr$^{-/-}$ macrophages were similar. This suggested that vesicular trafficking from the membrane to lysosomes and the enzymatic activity of ACAT were not impaired in beige,LDLr$^{-/-}$ macrophages.

Cholesterol efflux from macrophages can occur by passive aqueous diffusion (29), scavenger receptor class B type I-mediated uptake by HDL (30), and ABCA1-mediated active efflux of phospholipids and cholesterol (31). Cholesterol-enriched vesicles are routed to the plasma membrane and fuse to form cholesterol-rich rafts that donate cholesterol to the membrane. Early efflux time points should reflect membrane-derived cholesterol and late efflux time points should reflect lysosome-derived efflux. In the present studies, we assessed both short- and long-term efflux in cultured beige,LDLr$^{-/-}$ macrophages and found no cellular cholesterol efflux defects.

Neutrophils isolated from patients with CHS have impaired migration (18). Cellular migration could be compromised as a result of mechanical impediments resulting from the enlarged cytoplasmic granules. In vitro assessment of migration is sensitive to pore size. No migration defect was observed in beige neutrophils if the membrane pores were 8 μm in diameter (19). We measured macrophage invasion through a Matrigel®-coated membrane of 8 μm pores in response to JE/MCP-1. Matrigel® is a simulated basement membrane made primarily of laminin, but it also contains collagen IV (basement membrane-type collagen), heparin sulfate proteoglycans, entactin, and nidogen. Invasion of beige,LDLr$^{-/-}$ macrophage was reduced compared with that of LDL$^{-/-}$ macrophage, although the difference never reached statistical significance. Similar results were observed in response to the CXCR2 ligand, KC-Groα (data not shown), and this suggested that migration and invasion of beige,LDLr$^{-/-}$ macrophages may be attributable to the impaired digestion of matrix proteins as opposed to mechanical impediments.

The extracellular matrix of the arterial medium consists largely of type I and III fibrillar collagens (32). Atherosclerotic lesions consist largely of proteoglycans intermixed with loosely scattered collagen fibrils. Macrophages produce proteases that degrade extracellular matrix, including interstitial collagenases, stomelysin, and gelatinases such as MMP9 (33). Cultured beige,LDLr$^{-/-}$ macrophages secrete less pro-MMP9 activity compared with LDLr$^{-/-}$ macrophages. MMP9 is a secreted multidomain enzyme that is important in the remodeling of extracellular matrix and the invasion of cells (34). It cleaves denatured collagens (gelatin) and type IV collagen (basement membrane) and contributes to leukocyte tissue entry. Therefore, decreased MMP9 activity could affect macrophage distribution in beige,LDLr$^{-/-}$ lesions. If collagen degradation is impaired, the balance may be tipped toward matrix accumulation, and this could lead to a more stable lesion. It is important to note that zymography measures total enzyme activity and does not measure net activity, as would be relevant physiologically. For example, MMP9 is generally found bound by TIMP-1 and thus has no activity in vivo (33). The zymography characterized MMP activity. But the ELISA data suggested that the observed decreased activity of MMP9 was caused by impaired secretion of the enzyme. Furthermore, the Northern blot analysis suggested that the impairment includes reduced gene expression. It is important to mention, however, that we only performed this experiment using TNF-α as the agonist and cannot eliminate the possibility of impaired signaling through the TNF-α receptor.

In the present study, BMT study 1 was performed to determine the effect of beige macrophages on lesion morphology. In that experiment, only the bone marrow-derived cells of the LDLr$^{-/-}$ recipients expressed the beige mutation. Subsequently, we performed the inverse experiment in which beige,LDLr$^{-/-}$ mice were reconstituted with normal bone marrow (BMT study 2). In that study, all cells except those of bone marrow origin were mutant. We reported previously that beige,LDLr$^{-/-}$ double-mutant mice had greater lesion areas than LDLr$^{-/-}$ mice (2). Although we hypothesized that mice reconstituted with beige bone marrow would have greater disease severity, neither of these BMT studies resulted in exacerbated atherosclerosis. This substantiates our previous caveat (11) that direct comparisons between irradiated and nonirradiated mice are inappropriate. Nevertheless, BMT studies involving total body irradiation are informative when they are suitably controlled. Collectively, these studies confirmed that the exacerbated atherosclerosis of the double-mutant beige,LDLr$^{-/-}$ mice was not attributable solely to macrophages. This implies that cell types other than macrophages, including smooth muscle cells and endothelial cells, alone or in combination with macrophages, contribute to the increased lesion areas.

The cellular content of aortic sinus lesions was similar between LDLr$^{-/-}$ mice reconstituted with beige,GFP or wtGFP marrow. Also, beige,LDLr$^{-/-}$ mice reconstituted with mutant beige marrow had total GFP staining that was not significantly different from that of beige,LDLr$^{-/-}$ mice wild-type chimerae. Nevertheless, because all mice in studies 1 and 2 received irradiation and BMT, multiple conclusions were obtained by a comparison of BMT study 1 with BMT study 2. This comparison allowed us to identify the effects of the beige mutation in the BMT recipients. BMT recipients that expressed the beige mutation contained comparable numbers of macrophages, but those that were present appeared to be localized to the luminal surface. The same beige mutant recipient mice exhibited increased collagen staining and fewer necrotic cores. In conclusion, we documented that double-mutant beige,LDLr$^{-/-}$ mice have a unique stable-like lesion morphology characterized by increased collagen content and decreased macrophage infiltration. Importantly, this phenotype was not caused solely by aberrant macrophage function. Instead, this study confirms that other cell types, including smooth muscle cells and endothelial cells, likely contributed to the unique stable lesion morphology. This warrants additional study.

## REFERENCES

1. Dickson, B. C., and A. L. Gotlieb. 2003. Towards understanding acute destabilization of vulnerable atherosclerotic plaques. *Cardiovasc. Pathol.* **12:** 237–248.

2. Schiller, N. K., W. A. Boisvert, and L. K. Curtiss. 2002. Inflammation in atherosclerosis: lesion formation in LDL receptor-deficient mice with perforin and Lyst(beige) mutations. *Arterioscler. Thromb. Vasc. Biol.* **22:** 1341–1346.

3. Lutzner, M. A., C. T. Lowrie, and H. W. Jordan. 1967. Giant granules in leukocytes of the beige mouse. *J. Hered.* **58:** 299–300.

4. Ward, D. M., G. M. Griffiths, J. C. Stinchcombe, and J. Kaplan. 2000. Analysis of the lysosomal storage disease Chediak-Higashi syndrome. *Traffic.* **1:** 816–822.

5. Introne, W., R. E. Boissy, and W. A. Gahl. 1999. Clinical, molecular, and cell biological aspects of Chediak-Higashi syndrome. *Mol. Genet. Metab.* **68:** 283–303.

6. Nagle, D. L., M. A. Karim, E. A. Woolf, L. Holmgren, P. Bork, D. J. Misumi, S. H. McGrail, B. J. Dussault, Jr., C. M. Perou, R. E. Boissy, G. M. Duyk, R. A. Spritz, and K. J. Moore. 1996. Identification and mutation analysis of the complete gene for Chediak-Higashi syndrome. *Nat. Genet.* **14:** 307–311.

7. Frankel, F. R., R. W. Tucker, J. Bruce, and R. Stenberg. 1978. Fibroblasts and macrophages of mice with the Chediak-Higashi-like syndrome have microtubules and actin cables. *J. Cell Biol.* **79:** 401–408.

8. Wolff, S. M. 1972. The Chediak-Higashi syndrome: studies of host defenses. *Ann. Intern. Med.* **76:** 293–306.

9. Vassalli, J. D., A. Granelli-Piperno, C. Griscelli, and E. Reich. 1978. Specific protease deficiency in polymorphonuclear leukocytes of Chediak-Higashi syndrome and beige mice. *J. Exp. Med.* **147:** 1285–1290.

10. Mahoney, K. H., S. S. Morse, and P. S. Morahan. 1980. Macrophage functions in beige (Chediak-Higashi syndrome) mice. *Cancer Res.* **40:** 3934–3939.

11. Schiller, N. K., N. Kubo, W. A. Boisvert, and L. K. Curtiss. 2001. Effect of gamma-irradiation and bone marrow transplantation on atherosclerosis in LDL receptor-deficient mice. *Arterioscler. Thromb. Vasc. Biol.* **21:** 1674–1680.

12. Rady, P. L., P. Cadet, T. K. Bui, S. K. Tyring, S. Baron, G. J. Stanton, and T. K. Hughes. 1995. Production of interferon gamma messenger RNA by cells of non-immune origin. *Cytokine.* **7:** 793–798.

13. Yokoo, T., Y. Utsunomiya, T. Ohashi, T. Imasawa, T. Kogure, Y. Futagawa, T. Kawamura, Y. Eto, and T. Hosoya. 1998. Inflamed site-specific gene delivery using bone marrow-derived CD11b+CD18+ vehicle cells in mice. *Hum. Gene Ther.* **9:** 1731–1738.

14. Banka, C. L., A. S. Black, C. A. Dyer, and L. K. Curtiss. 1991. THP-1 cells form foam cells in response to coculture with lipoproteins but not platelets. *J. Lipid Res.* **32:** 35–43.

15. Curtiss, L. K., A. S. Black, Y. Takagi, and E. F. Plow. 1987. New mechanism for foam cell generation in atherosclerotic lesions. *J. Clin. Invest.* **80:** 367–373.

16. Markwell, M. A., S. M. Haas, L. L. Bieber, and N. E. Tolbert. 1978. A modification of the Lowry procedure to simplify protein determination in membrane and lipoprotein samples. *Anal. Biochem.* **87:** 206–210.

17. Rye, K-A., and P. J. Barter. 1994. The influence of apolipoproteins on the structure and function of spheroidal, reconstituted high density lipoproteins. *J. Biol. Chem.* **269:** 10298–10303.

18. Clark, R. A., and H. R. Kimball. 1971. Defective granulocyte chemotaxis in the Chediak-Higashi syndrome. *J. Clin. Invest.* **50:** 2645–2652.

19. Clawson, C. C., J. G. White, and J. E. Repine. 1978. The Chediak-Higashi syndrome. Evidence that defective leukotaxis is primarily due to an impediment by giant granules. *Am. J. Pathol.* **92:** 745–753.

20. Dollery, C. M., J. R. McEwan, and A. M. Henney. 1995. Matrix metalloproteinases and cardiovascular disease. *Circ. Res.* **77:** 863–868.

21. Loftus, I. M., and M. M. Thompson. 2002. The role of matrix metalloproteinases in vascular disease. *Vasc. Med.* **7:** 117–133.

22. Saren, P., H. G. Welgus, and P. T. Kovanen. 1996. TNF-alpha and IL-1beta selectively induce expression of 92-kDa gelatinase by human macrophages. *J. Immunol.* **157:** 4159–4165.

23. Kolodgie, F. D., A. P. Burke, A. Farb, H. K. Gold, J. Yuan, J. Narula, A. V. Finn, and R. Virmani. 2001. The thin-cap fibroatheroma: a type of vulnerable plaque: the major precursor lesion to acute coronary syndromes. *Curr. Opin. Cardiol.* **16:** 285–292.

24. Johnson, J. L., and C. L. Jackson. 2001. Atherosclerotic plaque rupture in the apolipoprotein E knockout mouse. *Atherosclerosis.* **154:** 399–406.

25. Rosenfeld, M. E., P. Polinsky, R. Virmani, K. Kauser, G. Rubanyi, and S. M. Schwartz. 2000. Advanced atherosclerotic lesions in the innominate artery of the ApoE knockout mouse. *Arterioscler. Thromb. Vasc. Biol.* **20:** 2587–2592.

26. Smith, J. D., E. Trogan, M. Ginsberg, C. Grigaux, J. Tian, and M. Miyata. 1995. Decreased atherosclerosis in mice deficient in both macrophage colony-stimulating factor (op) and apolipoprotein E. *Proc. Natl. Acad. Sci. USA.* **92:** 8264–8268.

27. Qiao, J. H., J. Tripathi, N. K. Mishra, Y. Cai, S. Tripathi, X. P. Wang, S. Imes, M. C. Fishbein, S. K. Clinton, P. Libby, A. J. Lusis, and T. B. Rajavashisth. 1997. Role of macrophage colony-stimulating factor in atherosclerosis: studies of osteopetrotic mice. *Am. J. Pathol.* **150:** 1687–1699.

28. Rajavashisth, T., J. H. Qiao, S. Tripathi, J. Tripathi, N. Mishra, M. Hua, X. P. Wang, A. Loussararian, S. Clinton, P. Libby, and A. Lusis. 1998. Heterozygous osteopetrotic (op) mutation reduces atherosclerosis in LDL receptor-deficient mice. *J. Clin. Invest.* **101:** 2702–2710.

29. Rothblat, G. H., M. Llera-Moya, V. Atger, G. Kellner-Weibel, D. L. Williams, and M. C. Phillips. 1999. Cell cholesterol efflux: integration of old and new observations provides new insights. *J. Lipid Res.* **40:** 781–796.

30. Ji, Y., B. Jian, N. Wang, Y. Sun, M. L. Moya, M. C. Phillips, G. H. Rothblat, J. B. Swaney, and A. R. Tall. 1997. Scavenger receptor BI promotes high density lipoprotein-mediated cellular cholesterol efflux. *J. Biol. Chem.* **272:** 20982–20985.

31. Wang, N., D. L. Silver, P. Costet, and A. R. Tall. 2000. Specific binding of ApoA-I, enhanced cholesterol efflux, and altered plasma membrane morphology in cells expressing ABC1. *J. Biol. Chem.* **275:** 33053–33058.

32. Ross, R. 1999. Atherosclerosis—an inflammatory disease. *N. Engl. J. Med.* **340:** 115–126.

33. Opdenakker, G., P. E. Van den Steen, and J. Van Damme. 2001. Gelatinase B: a tuner and amplifier of immune functions. *Trends Immunol.* **22:** 571–579.

34. Nagase, H., and J. F. Woessner, Jr. 1999. Matrix metalloproteinases. *J. Biol. Chem.* **274:** 21491–21494.